tvst
Artificial Intelligence

Quantitative Assessment of Fundus Tessellated Density in Highly Myopic Glaucoma Using Deep Learning

Xiaohong Chen[1,*], Xuhao Chen[1,*], Jianqi Chen[1,*], Zhidong Li[1], Shaofen Huang[1], Xinyue Shen[1], Yue Xiao[1], Zhenquan Wu[2], Yingting Zhu[1], Lin Lu[1], and Yehong Zhuo[1]

[1] State Key Laboratory of Ophthalmology, Zhongshan Ophthalmic Center, Sun Yat-Sen University, Guangdong Provincial Key Laboratory of Ophthalmology and Visual Science, World Health Organization Collaborating Center for Eye Care and Vision, Guangzhou, China
[2] Shenzhen Eye Hospital, Jinan University, Shenzhen Eye Institute, Shenzhen, China

Correspondence: Yehong Zhuo, State Key Laboratory of Ophthalmology, Zhongshan Ophthalmic Center, Sun Yat-Sen University, Guangdong Provincial Key Laboratory of Ophthalmology and Visual Science, World Health Organization Collaborating Center for Eye Care and Vision, No. 7 Jinsui Road, Tianhe District, Guangzhou 510060, China. e-mail: zhuoyh@mail.sysu.edu.cn
Lin Lu, State Key Laboratory of Ophthalmology, Zhongshan Ophthalmic Center, Sun Yat-Sen University, Guangdong Provincial Key Laboratory of Ophthalmology and Visual Science, World Health Organization Collaborating Center for Eye Care and Vision, No. 7 Jinsui Road, Tianhe District, Guangzhou 510060, China. e-mail: lvlin@mail.sysu.edu.cn
Yingting Zhu, State Key Laboratory of Ophthalmology, Zhongshan Ophthalmic Center, Sun Yat-Sen University, Guangdong Provincial Key Laboratory of Ophthalmology and Visual Science, World Health Organization Collaborating Center for Eye Care and Vision, No. 7 Jinsui Road, Tianhe District, Guangzhou 510060, China. e-mail: zhuyt35@mail.sysu.edu.cn

Received: October 25, 2023
Accepted: January 12, 2024
Published: April 9, 2024

Keywords: high myopia; glaucoma; fundus photograph; fundus tessellation; deep learning

Purpose: To characterize the fundus tessellated density (FTD) in highly myopic glaucoma (HMG) and high myopia (HM) for discovering early signs and diagnostic markers.

Methods: This retrospective cross-sectional study included hospital in-patients with HM (133 eyes) and HMG (73 eyes) with an axial length $\geq$26 mm at Zhongshan Ophthalmic Center. Using deep learning, FTD was quantified as the average exposed choroid area per unit area on fundus photographs in the global, macular, and disc regions. FTD-associated factors were assessed using partial correlation. Diagnostic efficacy was analyzed using the area under the curve (AUC).

Results: HMG patients had lower global (0.20 $\pm$ 0.12 versus 0.36 $\pm$ 0.09) and macular FTD (0.25 $\pm$ 0.14 vs. 0.40 $\pm$ 0.09) but larger disc FTD (0.24 $\pm$ 0.11 vs. 0.19 $\pm$ 0.07) than HM patients in the tessellated fundus (all $P < 0.001$). In the macular region, nasal FTD was lowest in the HM (0.26 $\pm$ 0.13) but highest in the HMG (0.32 $\pm$ 0.13) compared with the superior, inferior, and temporal subregions (all $P < 0.05$). A fundus with a macular region nasal/temporal (NT) FTD ratio > 0.96 (AUC $= 0.909$) was 15.7 times more indicative of HMG than HM. A higher macular region NT ratio with a lower horizontal parapapillary atrophy/disc ratio indicated a higher possibility of HMG than HM (AUC $= 0.932$).

Conclusions: FTD differs in degree and distribution between HMG and HM. A higher macular NT alone or with a lower horizontal parapapillary atrophy/disc ratio may help differentiate HMG.

Translational Relevance: Deep learning-based FTD measurement could potentially assist glaucoma diagnosis in HM.

Citation: Chen X, Chen X, Chen J, Li Z, Huang S, Shen X, Xiao Y, Wu Z, Zhu Y, Lu L, Zhuo Y. Quantitative assessment of fundus tessellated density in highly myopic glaucoma using deep learning. Transl Vis Sci Technol. 2024;13(4):17, https://doi.org/10.1167/tvst.13.4.17

Introduction

High myopia (HM) is the leading vision-threatening disease among working-age populations worldwide. Furthermore, its prevalence is projected to reach approximately 1 billion by 2050.[1] HM is also a major risk factor for developing glaucoma.[2] However, the diagnosis of highly myopic glaucoma (HMG) can be difficult, especially in the preliminary stages, because of uneventful intraocular pressure (IOP), atypical glaucomatous optic neuropathy (GON), and visual field (VF) defects caused by myopic fundus structural reconstruction.[3–6]

Fundus tessellation (FT), the earliest and most common fundus manifestation of HM, is associated with the development and progression of myopic macular degeneration.[7–10] However, to date, few studies have investigated the characteristics of FT in HMG. Moreover, there are no reports on whether the degree and distribution of FT are the same between the HM and HMG fundi. In a hospital-based study, Spaeth et al.[11] reported that a higher FT was associated with open-angle glaucoma (OAG) with shallow glaucomatous cupping, a type of age-related atrophic OAG. Similarly, Yan et al.[12] found an association between FT and a higher glaucoma prevalence in the Beijing Eye Study. However, none of these studies mentioned the differences when combined with HM. Therefore exploring FT characteristics may be critical in discovering early signs and diagnostic markers for HMG.

A major limitation in FT evaluation in the past was qualitative or semi-qualitative assessments, depending largely on the experience and understanding of ophthalmologists, which might have resulted in controversial conclusions among studies. However, with the development of artificial intelligence, FT is easily identified on fundus photographs as part of HM diagnosis.[13,14] However, at this stage, the evaluation of FT by machine learning is still qualitative but more objective. Furthermore, recent advances in deep learning can quantitatively assess FT by extracting the exposed choroid on fundus images and calculating the average exposed choroid area per unit area of the fundus, named fundus tessellated density (FTD).[15] Recent studies have also shown that FTD is negatively correlated with subfoveal choroidal and retinal nerve fiber layer thickness and positively correlated with age, axial length (AL), parapapillary atrophy (PPA) area, vessel density inside the optic disc, and vertical diameter of the optic disc.[15–18] These results are similar to those of qualitative studies on FT, demonstrating the reliability of FTD as an index for assessing FT in association with other ocular and systemic parameters.[12]

Therefore, in the present study, we aimed to use FTD to quantitatively investigate FT characteristics in HM and HMG fundus by describing their distribution patterns. We also evaluated relationships between FTD and other associated factors to identify biomarkers with early diagnostic value for HM and HMG.

Methods

Study Design and Participants

This retrospective cross-sectional study included in-hospital patients diagnosed with HM or HMG at the Zhongshan Ophthalmic Center (Guangzhou, China). Patients with HM were recruited from the Retina Department between January 2019 and January 2021, and patients with HMG were recruited from the Glaucoma Department between November 2018 and March 2022. This study was approved by the Ethics Committee of the Zhongshan Ophthalmic Center (No. 2022KYPJ105) and followed the principles of the Declaration of Helsinki. The requirement for informed consent was waived because of the retrospective nature of the study and data de-identification. Only patients with available color fundus photographs were included in the study. The right eye of each patient was used for the analysis to reduce a high correlation with the fellow eye. If only one eye was available, that eye was included.

Inclusion and Exclusion Criteria

This study recruited adult patients aged >18 years. Based on the META-analysis for Pathologic Myopia

classification system for myopic maculopathy, category 1 (tessellated fundus) and category 2 (diffuse chorioretinal atrophy) fundus were included in the analysis.[10] The exclusion criteria were inherited diseases, congenital eye diseases, ocular infections, trauma, ischemia, compressive optic neuropathy, optic neuritis, retinal detachment, macular hole, retinal schisis, retinal vessel occlusion, vitreous hemorrhage, age-related macular degeneration, vitreoretinal surgery, or any ocular disease involving lesions in the optic nerve or macula. Additionally, images with optic media opacities, insufficient image quality, or medical records with missing key variables were excluded. Fundus images were independently reviewed by two experienced ophthalmologists (X.C. and Y.Z.) in a masked manner to meet the inclusion and exclusion criteria. Any controversies regarding the diagnosis were resolved by a senior ophthalmologist (Z.H.).

Ophthalmological Examinations

All included patients had complete medical records, including age, sex, and comprehensive eye examination results using anterior slit-lamp microscopy, Goldmann applanation tonometry (Haag-Streit, Bern, Switzerland), gonioscopy, dilated fundus examination, AL measurement (IOL Master 700; Carl Zeiss Meditec AG, Jena, Germany), and VF test with a standard 30–2 Swedish interactive threshold algorithm (Humphrey Field Analyzer, Model 750; Carl Zeiss Meditec AG). Color fundus photographs were taken at 45°, centered on the macula, using fundus cameras (Kowa Nonmyd WX; Kowa Inc., Nagoya, Japan; and DRI-OCT, Triton; Topcon, Tokyo, Japan). Optical coherence topography (OCT) images were acquired for all the patients participated (Heidelberg Engineering, Heidelberg, Germany; and DRI-OCT Triton, Topcon). The reliability of the VF test results was monitored as follows: number of fixation losses $\leq 20\%$, rate of false-negative results $\leq 33\%$, and rate of false-positive results $\leq 33\%$.

Definitions

In this study, HM was defined by an AL $\geq$ 26.00 mm.[19,20] HMG was the diagnosis of OAG with an AL $\geq$ 26.00 mm. OAG was identified based on GON characteristics, including rim thinning in the inferotemporal and superotemporal quadrants, excavation, notching, cup enlargement, retinal nerve fiber layer defects, glaucomatous VF loss that could not be explained by other reasons, and an open anterior chamber on gonioscopy.[21,22] For those suspect of glaucomatous ONH, standardized stereoscopic photographs of the optic disc were acquired for differentiation. Besides, all the patients had OCT images for further validation of ONH deformation. Glaucomatous damage on the VF was identified by (1) at least two fields in a hemifield test outside normal limits, (2) three or more non-edge points with a pattern deviation plot at a $P < 5\%$ level in a typical glaucomatous area and one with a $P < 1\%$ level on two consecutive fields, or (3) a corrected pattern standard deviation in $<5\%$ of normal fields on two consecutive fields.[23]

Fundus Parameters and Fundus Tessellated Density Quantification With Deep Learning

As described in previous studies,[15,17] parameters were extracted from fundus photographs and quantitatively assessed using deep learning-based technology (EVisionAI, EVision Technology Co., Ltd., Beijing, China). In brief, fundus images underwent preprocessing including region-of-interest extraction, denoising, normalization, and enhancement to enable consistency for analysis. Sample labeling was carried out automatically and then corrected manually. The software automatically identified the optic disc center and macular foveola based on their visual attention mechanisms. Their segmentation was based on the Resnet-FCN, a deep learning semantic segmentation network and edge extraction algorithm.[15] Based on this segmentation, FTD and other parameters including optic disc, PPA, and retinal vessels were automatically measured.[15–18,24–27]

FTD was calculated as the average exposed choroid area per unit area of the fundus.[15–18] FTD in the global fundus, macular region (a 6 mm-diameter circle centered on the foveola), and disc region (a 4.5 mm-diameter circle centered on the optic disc center) were measured separately (Figs. 1A–C). The macular and disc regions were further divided to measure the sectoral FTD using three approaches: semicircles (upper and lower), X-shaped quadrants (superior, inferior, nasal, and temporal), and coordinate quadrants (superonasal [SN], superotemporal [ST], inferonasal [IN], and inferotemporal [IT]) (Figs. 1D–F). The vertical PPA/disc ratio (VPDR) and the horizontal PPA/disc ratio (HPDR) are the ratios of the PPA diameter to the disc diameter on the vertical and horizontal axes, respectively. The PPA/disc area ratio (PDAR) is the ratio of the PPA area to the disc area. The vertical cup/disc ratio (VCDR) is the ratio of the cup diameter to the disc diameter on the vertical axis. Disc ovality index (DOI) is the ratio of the long axis to the short axis of the smallest circumscribed ellipse of the optic disc. The disk becomes

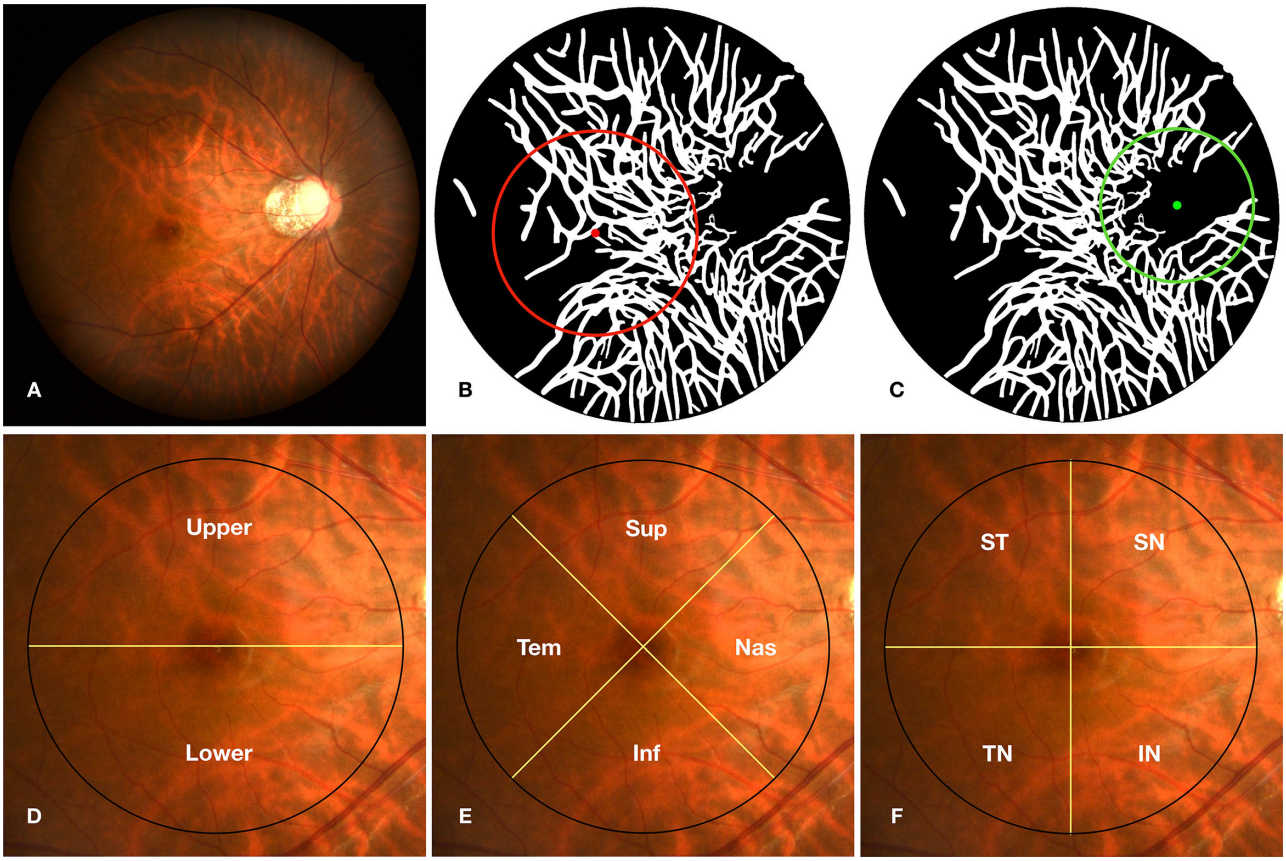

Figure 1. Quantification of FTD on fundus photographs with deep learning. The original fundus photograph (**A**) was preprocessed, and the FTD in the macular region (6 mm, *red circle*, (**B**) and disc region (4.5 mm, *green circle*, (**C**) were quantified using deep learning. The macular and disc regions were further divided using (**D**) semicircles (upper and lower); (**E**) X-shaped quadrants (Sup, Inf, Nas, and Tem); and (**F**) coordinate quadrants (SN, ST, IN, and IT). Sup, superior; Inf, inferior; Nas, nasal; Tem, temporal; SN, superonasal; ST, superotemporal; IN, inferonasal; IT, inferotemporal.

more circular as the DOI approaches 1. Retinal vessel density (RVD) is the entire vessel area in a certain unit area.

Statistical Analysis

Statistical analyses were performed using SPSS software (v26.0, IBM Corp., Armonk, NY, USA). Data are presented as mean ± standard deviation for continuous variables and counts (percentage) for categorical variables. Comparisons between the two groups were performed using the Student's t test or χ^2 test. For fundus and FTD parameters between the groups, the statistical analysis was adjusted for age, sex, AL, and IOP. Multiple groups were compared using one-way analysis of variance with Bonferroni correction for post hoc tests. Bar graphs are expressed as mean ± standard error. Partial correlation analysis was performed to study the associations between FTD and other parameters by adjusting for age, AL, and IOP and expressed as the correlation coefficient r (P value). Venn diagrams were used to illustrate the correlations between groups and regions. Scatter plots and locally weighted smoothing fitting lines were used for visualization. Logistic regression analysis was performed to explore the factors associated with differences between the HM and HMG groups. Receiver operating characteristic curves and the areas under the curve (AUCs) were analyzed to evaluate the diagnostic efficiencies of the multivariate models. $P \leq 0.05$ was considered statistically significant.

Results

Demographic and Ocular Characteristics

In total, 206 patients (206 eyes) were included in the final analysis, including 133 eyes with HM and 73 eyes with HMG. As presented in Table 1, compared with the HM group, the HMG group had younger age, more men, higher IOP, shorter AL, lower VPDR, HPDR,

Table 1. Demographic and Ocular Characteristics in High Myopia and Highly Myopic Glaucoma Groups

	All Subjects ($n = 206$ Eyes)			Category 1[a] ($n = 166$ Eyes)			Category 2[a] ($n = 40$ Eyes)		
	HM ($n = 133$)	HMG ($n = 73$)	*P* Value[*]	HM ($n = 99$)	HMG ($n = 67$)	*P* Value[*]	HM ($n = 34$)	HMG ($n = 6$)	*P* Value[*]
Demographic parameters									
Age (years)	47 ± 12	42 ± 13	**0.008**	46 ± 11	41 ± 12	**0.016**	50 ± 13	51 ± 17	0.848
Sex (Male, %)	41 (30.8%)	55 (75.3%)	**<0.001**	28 (28.3%)	51 (76.1%)	**<0.001**	13 (38.2%)	4 (66.7%)	0.194
Ocular parameters									
AL (mm)	29.50 ± 1.82	27.88 ± 2.00	**<0.001**	29.02 ± 1.51	27.56 ± 1.53	**<0.001**	30.89 ± 1.94	31.40 ± 3.21	0.594
IOP (mm Hg)	15.5 ± 2.9	20.8 ± 9.2	**<0.001**	15.5 ± 2.5	21.0 ± 9.3	**<0.001**	15.4 ± 3.9	19.0 ± 8.0	0.320
Fundus parameters									
VPDR	1.68 ± 0.44	1.29 ± 0.33	**<0.001**	1.62 ± 0.41	1.26 ± 0.29	**0.003**	1.89 ± 0.47	1.61 ± 0.59	0.058
HPDR	1.31 ± 0.61	0.56 ± 0.37	**<0.001**	1.24 ± 0.57	0.50 ± 0.30	**<0.001**	1.55 ± 0.67	1.27 ± 0.43	0.135
PDAR	3.31 ± 2.24	1.22 ± 1.34	**<0.001**	2.91 ± 1.83	1.01 ± 0.83	**<0.001**	4.54 ± 2.88	3.58 ± 3.08	0.211
VCDR	0.38 ± 0.08	0.57 ± 0.14	**<0.001**	0.38 ± 0.08	0.57 ± 0.14	**<0.001**	0.38 ± 0.08	0.53 ± 0.20	**0.004**
DOI	0.68 ± 0.12	0.81 ± 0.11	**<0.001**	0.68 ± 0.12	0.82 ± 0.09	**<0.001**	0.67 ± 0.10	0.62 ± 0.13	0.237
RVD	0.060 ± 0.016	0.062 ± 0.020	**<0.001**	0.063 ± 0.016	0.065 ± 0.019	**<0.001**	0.050 ± 0.011	0.034 ± 0.009	**0.002**
FTD									
Global fundus	0.35 ± 0.09	0.20 ± 0.11	**<0.001**	0.36 ± 0.09	0.20 ± 0.12	**<0.001**	0.33 ± 0.08	0.18 ± 0.06	**<0.001**
Macular region[b]	0.37 ± 0.11	0.24 ± 0.14	**<0.001**	0.40 ± 0.09	0.25 ± 0.14	**0.003**	0.28 ± 0.12	0.14 ± 0.06	**0.017**
Disc region	0.18 ± 0.07	0.23 ± 0.11	**0.001**	0.19 ± 0.07	0.24 ± 0.11	**<0.001**	0.14 ± 0.08	0.15 ± 0.09	0.679
MD ratio	2.07 ± 1.28	1.61 ± 1.07	0.078	2.34 ± 1.03	1.04 ± 0.49	**<0.001**	2.23 ± 1.07	1.46 ± 1.50	0.182

Data are presented as mean ± standard deviation or counts (percentage).

[a]Category 1 (tessellated fundus) and Category 2 (diffuse choroidal atrophy) were classified according to META-PM classification.

[b]Macular region: a 6 mm-diameter circle centered on the foveola; Disc region: a 4.5 mm-diameter circle centered on the optic disc center.

[*]For fundus and FTD parameters, p value was adjusted for age, sex, AL and IOP. *P* value was marked bold as $P < 0.05$.

and PDAR, and higher VCDR, DOI, and RVD (all $P < 0.008$). In the Category 1 fundi, similar trends were observed in the demographic, ocular, and fundus parameters between the HMG and HM groups (all $P \leq 0.016$). In the Category 2 fundi, the parameters were comparable between the two groups (all $P > 0.05$); however, a larger VCDR and lower RVD were observed in the HMG group (both $P \leq 0.004$).

Fundus Tessellated Density Characteristics in the Global and Regional Fundus

Generally, the HMG group had lower global and macular FTD (both $P < 0.001$), although the disc FTD was slightly higher ($P = 0.001$) than the HM group (Table 1). Fundus FTD in Category 1 fundi had a similar pattern between the HMG and HM groups (all $P \leq 0.003$), whereas disc FTD between the two groups was comparable in Category 2 fundi ($P = 0.679$). To explore the relationship between the macular and disc FTD within the same fundus, we determined the macular FTD/disc FTD (MD) ratio. A significantly higher MD ratio was observed in the HM group (2.34 ± 1.03) compared with the HMG group (1.04 ± 0.49) only in the Category 1 fundi ($P < 0.001$). Thus Category 1 fundi were further analyzed.

Fundus Tessellated Density Distribution in High Myopia and Highly Myopic Glaucoma Groups

FTD distribution in different fundus sectors is presented in Figure 2 and Supplementary Table S1. The FTD in the lower semicircle was higher than that in the upper semicircle ($P = 0.002$) in the disc region of HMG eyes (Fig. 2B). Within the X-shaped quadrants, the nasal FTD was the lowest in the HM but the largest in the HMG group compared with the superior, inferior, and temporal sectors (all $P \leq 0.032$, Fig. 2C) in the macular region. Temporal FTD was lower compared with inferior and superior quadrants (both $P \leq 0.003$) in the HMG group. We evaluated the nasal FTD/temporal FTD (NT) ratio in the macular region and found it to be significantly lower in the HM group (0.69 ± 0.50) than in the HMG group (4.87 ± 6.50, $P < 0.001$) after adjusting for age, sex, AL and IOP. In the disc region, FTD in the inferior and temporal sectors was higher than that in the superior and nasal sectors in the HMG group (all $P \leq 0.002$, Fig. 2D). Furthermore, we assessed the inferior FTD/superior FTD (IS) ratio in the disc region and found statistical differences between the HM (1.24 ± 1.63) and HMG groups (2.26 ± 2.54; $P = 0.006$). However, the differences were not

Table 2. Correlation Analysis Between Fundus Tessellated Density and Ocular Parameters in Tessellated Fundus Expressed as *r* (*P*)

	Age	IOP	AL	VPDR[a]	HPDR[a]	PDAR[a]	VCDR[a]	DOI[a]	RVD[a]
HM group									
Global fundus	**0.371 (<0.001)**	−0.186 (0.066)	**0.264 (0.008)**	**0.216 (0.039)**	0.163 (0.120)	0.148 (0.160)	−0.056 (0.598)	−0.142 (0.177)	**−0.497 (<0.001)**
MD Ratio	0.189 (0.064)	**−0.233 (0.023)**	**0.260 (0.010)**	0.202 (0.054)	**0.292 (0.005)**	**0.290 (0.005)**	−0.082 (0.435)	−0.103 (0.327)	0.026 (0.809)
Macular region[b]	**0.287 (0.004)**	−0.183 (0.072)	0.154 (0.129)	0.177 (0.91)	**0.206 (0.049)**	0.180 (0.086)	−0.099 (0.346)	**−0.209 (0.046)**	**−0.484 (<0.001)**
NT Ratio	**−0.348 (<0.001)**	0.073 (0.479)	**−0.480 (<0.001)**	**−0.276 (0.009)**	**−0.343 (0.001)**	**−0.330 (0.002)**	0.205 (0.053)	**0.225 (0.033)**	**0.271 (0.010)**
Disc region[c]	−0.022 (0.830)	0.105 (0.309)	−0.149 (0.146)	−0.187 (0.075)	−0.187 (0.075)	**−0.256 (0.014)**	0.074 (0.484)	−0.068 (0.518)	**−0.268 (0.010)**
IS Ratio	**−0.276 (0.007)**	0.175 (0.093)	−0.202 (0.051)	−0.068 (0.523)	0.022 (0.840)	0.001 (0.994)	−0.032 (0.766)	−0.052 (0.628)	**0.318 (0.002)**
HMG group									
Global fundus	**0.374 (0.002)**	−0.182 (0.141)	**0.497 (<0.001)**	**0.259 (0.039)**	−0.005 (0.966)	0.031 (0.807)	0.121 (0.339)	0.064 (0.613)	−0.166 (0.190)
MD Ratio	0.203 (0.100)	−0.004 (0.976)	**0.511 (<0.001)**	0.224 (0.076)	0.240 (0.056)	0.227 (0.072)	0.061 (0.630)	−0.237 (0.059)	−0.008 (0.950)
Macular region[b]	**0.333 (0.006)**	−0.181(0.142)	**0.552 (<0.001)**	**0.248 (0.048)**	0.082 (0.518)	0.085 (0.502)	0.155 (0.222)	−0.070 (0.583)	−0.178 (0.158)
NT Ratio	**−0.265 (0.039)**	0.121 (0.353)	−0.152 (0.242)	−0.060 (0.656)	−0.032 (0.812)	−0.073 (0.585)	0.004 (0.975)	0.088 (0.510)	−0.057 (0.668)
Disc region[c]	**0.267 (0.029)**	**−0.305 (0.012)**	0.213 (0.084)	0.152 (0.229)	−0.108 (0.395)	−0.084 (0.512)	0.093 (0.466)	0.190 (0.133)	−0.174 (0.168)
IS Ratio	**−0.278 (0.026)**	0.218 (0.083)	**−0.287 (0.021)**	**−0.325 (0.011)**	−0.116 (0.375)	−0.133 (0.308)	−0.036 (0.785)	−0.070 (0.591)	0.002 (0.985)

IS ratio, inferior FTD/superior FTD ratio. *P* values marked bold <0.05.

[a]Partial correlation by adjusting age, AL and IOP.

[b]Macular region is the circle of 6 mm diameter centered on the foveola.

[c]Disc region is the circle of 4.5 mm diameter centered on the optic disc center.

Table 3. Logistic Regression Analysis of Parapapillary Atrophy and Fundus Tessellated Density Between High Myopia and Highly Myopic Glaucoma

	Univariate Model		Multivariate Model (Adjust Age, Sex, IOP and AL)	
	OR (95% CI)	*P* Value	OR (95% CI)	*P* Value
VPDR	23.348 (6.861∼79.455)	<0.001	10.139 (1.493∼68.865)	0.018
HPDR	83.228 (19.638∼352.719)	<0.001	87.518 (11.148∼687.149)	<0.001
PDAR	3.545 (2.253∼5.580)	<0.001	4.276 (1.991∼9.183)	<0.001
Global FTD	8.8×10^5 (1.4×10^4∼5.5×10^7)	<0.001	2.2×10^4 (68.326∼7.2×10^6)	0.001
Macular FTD	4.1×10^4 (1.2×10^3∼1.4×10^6)	<0.001	216.055 (2.057∼2.3×10^4)	0.024
Disc FTD	883.6 (19.5∼4.0×10^4)	<0.001*	1.8×10^4 (71.077∼4.5×10^6)	0.001*
MD ratio	17.238 (7.096∼41.878)	<0.001	12.695 (3.941∼40.890)	<0.001
NT ratio	9.787 (4.392∼21.813)	<0.001*	10.698 (3.131∼36.552)	0.001*
IS ratio	1.344 (1.070∼1.689)	0.011*	0.997 (0.786∼1.265)	0.980*

IS ratio, Inferior FTD/superior FTD ratio.
*HM was set as the reference.

Table 4. Logistic Regression of Macular Nasal/Temporal Ratio Between High Myopia and Highly Myopic Glaucoma

	Univariable Model		Multivariable Model	
	OR (95% CI)	*P* Value	OR (95% CI)	*P* Value
NT ratio (≥0.96 vs. <0.96)	33.175 (12.559, 87.633)	<0.001	15.684 (4.205, 58.493)	<0.001

CI, confidence interval; NT ratio, nasal FTD/temporal FTD ratio; OR, odds ratio.
Multivariable model is adjusted for age, sex, AL, and IOP.

statistically significant after adjusting for age, sex, AL, and IOP ($P = 0.917$). The FTD distribution patterns within the coordinate quadrants were similar to those within the X-shaped quadrants (Figs. 2E, 2F). Therefore an X-shaped quadrant was used in subsequent analyses.

Associations Between Fundus Tessellated Density and Other Biometric Parameters

FTD and its associated factors were evaluated as presented in Table 2. In both groups, larger global FTD was associated with older age, longer AL, and larger VPDR (all $P < 0.05$). Larger macular FTD was associated with older age (both $P \leq 0.006$); however, no shared factors were associated with disc FTD in either group (all $P > 0.05$). The Venn diagrams demonstrate these associations (Fig. 3). According to the scatter plots, the trends for global, macular, and disc FTDs between the HM and HMG groups were relatively stable as AL increased (Figs. 4A–C). Therefore we did not further analyze the subgroups according to AL. Disc FTD was negatively correlated with IOP in the HMG group, but not in the HM group (Fig. 4D). In addition, FTD and its associated factors in each sector within the X-shaped quadrant were analyzed, as illustrated in Supplementary Table S2 and Supplementary Figure S1.

Fundus Tessellated Density as a Differential Index for Identifying Glaucoma in High Myopia

To identify the differential parameters between the HM and HMG groups, FTD and PPA were analyzed using univariate and multivariate logistic regression analyses, respectively. As presented in Table 3, most of these parameters exhibited different abilities. The AUC was further analyzed to evaluate the differential efficiencies. Among the FTD-related parameters, the NT ratio had the highest AUC (0.909) (Figs. 5A, 5B). The cutoff value for the NT ratio was 0.96 (sensitivity, 0.902; specificity, 0.784). Therefore a fundus photograph with an NT ratio higher than 0.96 was 15.7 times more likely to be of HMG than of HM (Table 4). Moreover, the highest AUC for PPA related parameters was HPDR (0.890), with a cutoff value of 0.81 (sensitivity, 0.740; specificity, 0.925) (Fig. 5C). Furthermore, the combination of NT ratio with HPDR

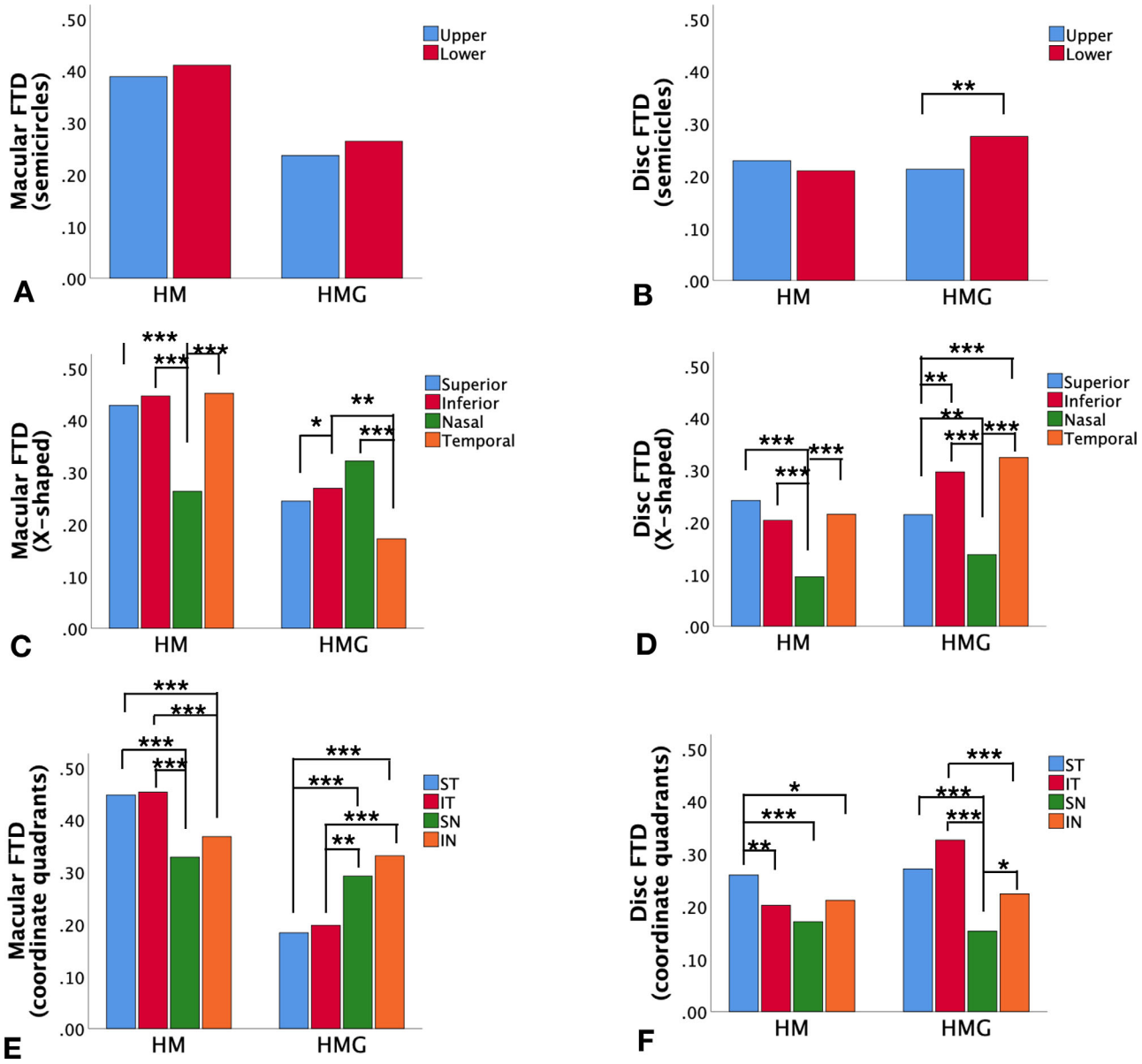

Figure 2. FTD distribution in the macular and disc regions. The FTD in the HM and HMG groups were further analyzed using (**A**) semicircles (upper and lower) in the macular region; (**B**) semicircles (upper and lower) in the disc region; (**C**) X-shaped quadrants (superior, inferior, nasal, and temporal) in the macular region; (**D**) X-shaped quadrants (superior, inferior, nasal, and temporal) in the disc region; (**E**) coordinate quadrants (SN, ST, IN, and IT) in the macular region; and (**F**) coordinate quadrants (SN, ST, IN, and IT) in the disc region. SN, superonasal; ST, superotemporal; IN, inferonasal; IT, inferotemporal. *$P < 0.05$, **$P < 0.01$, ***$P < 0.001$.

achieved the highest AUC of 0.932 (sensitivity, 0.869; specificity, 0.872) for distinguishing HMG from HM (Fig. 5D).

Discussion

In this study, we quantified FTD and evaluated its intensity, distribution, associated factors, and diagnostic ability in HM and HMG. In the Category 1 fundi, HMG eyes had a lower global FTD and MD ratio, but a higher macular NT ratio than HM eyes. In both groups, shared factors associated with global FTD were age, AL, and VPDR. However, age alone was associated with macular FTD. Moreover, a negative IOP-disc FTD correlation was found in HMG eyes only. For a single index, a macular NT ratio higher than 0.96 had 15.7 times possibility of being HMG rather than HM. For complex indexes, a higher macular NT ratio with a lower HPDR indicated a higher possibility of HMG than of HM. To the best of our

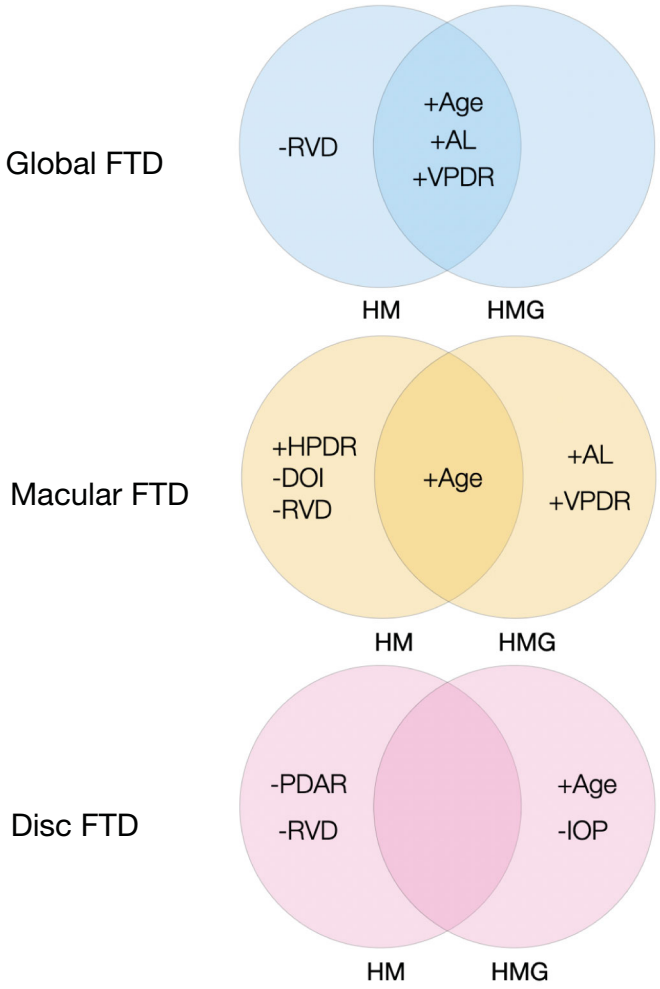

Figure 3. Venn diagrams showing FTD and associated factors in HM and HMG groups in the global, macular, and disc regions.

knowledge, such findings have not been previously reported.

We found lower global and macular FTD in eyes with HMG compared with eyes with HM. In addition, we observed a positive AL-global FTD correlation in both groups, and a positive AL-macular FTD correlation in eyes with HMG. Previous studies have reported comparable results, showing that increasing AL is associated with a higher degree of FT, mainly due to the thinning of the choriocapillaris as the eye elongates.[12,15,28,29] However, differences in FTD between HM and HMG have not been previously reported. Based on previous investigations, the increased ophthalmoscopic visibility of the FT is known to be associated with increased transparency of the retinal pigment epithelium and choriocapillaris, less filling in the choriocapillaris, increased pigmentation of the intrachoroidal regions associated with ethnicity, and choroid thinning.[28–34] Therefore one postulation is that the thinning speed of the retina and choroid is faster in eyes with HM than in eyes with HMG. This was supported by an optical coherence tomography angiography study showing slightly higher average choroidal thickness in an HM group with primary OAG (183.5 $\pm$ 63.5) than in an HM group without primary OAG (171.1 $\pm$ 54.7) and a significantly higher capillary density of choriocapillaris in the HM group with primary OAG (54.8 $\pm$ 0.60) compared with the HM group without primary/ OAG (54.5 $\pm$ 0.65, $P <$ 0.001).[35] The present results supported this hypothesis by showing slightly higher retinal vessel density in the HMG group than in the HM group (Table 1).

Furthermore, the present study revealed different FTD distribution patterns in HM and HMG, as macular nasal FTD was lowest in the HM fundus and highest in the HMG fundus. Notably, the macular NT ratio, which was significantly higher in eyes with HMG than in eyes with HM, achieved the best differential efficiency between the two groups. Further evaluation of the nasal region showed advanced atrophy and exposure of the sclera more commonly in HM eyes and less frequently in HMG eyes (evaluated by L.L). A previous study by Yoshihara et al.[30] reported a significant correlation between a higher FT and a thinner nasal choroid in young healthy Japanese individuals. However, the association of FT with other regions, such as the temporal, superior, or inferior choroid, was not investigated. Therefore, we postulate that the nasal region may be the earliest area of myopic degenerative changes in the pathophysiological process. This degenerative process develops faster in eyes with HM than in eyes with HMG, thus making atrophy in the nasal region in eyes with HM more common than in eyes with HMG. Notably, FTD was not always accurate in determining the severity of myopic degeneration.

We also found a negative IOP–disc FTD correlation in eyes with HMG and a negative IOP–MD ratio and marginally negative IOP–macular FTD correlation ($r = -0.183$, $P = 0.072$) in eyes with HM. These results slightly differed from those of previous studies showing no association between the FT degree and IOP.[12] Yan et al.[12] reported a higher degree of macular FT with a higher prevalence of GON in their population-based study, which they connected to an atrophic type of primary OAG with relatively low IOP or the "atrophic glaucoma" proposed by Spaeth,[11] characterized by a large PPA beta zone and shallow glaucomatous cupping.[34] However, the study of atrophic OAG was conducted in older individuals with refractive errors of less than −8 diopters, which was different from the present study participants. Thus, owing to differences in AL, health or disease status, population- or hospital-based scenarios, or ethnicities explain the discrepancy between our results and those of previous studies. An

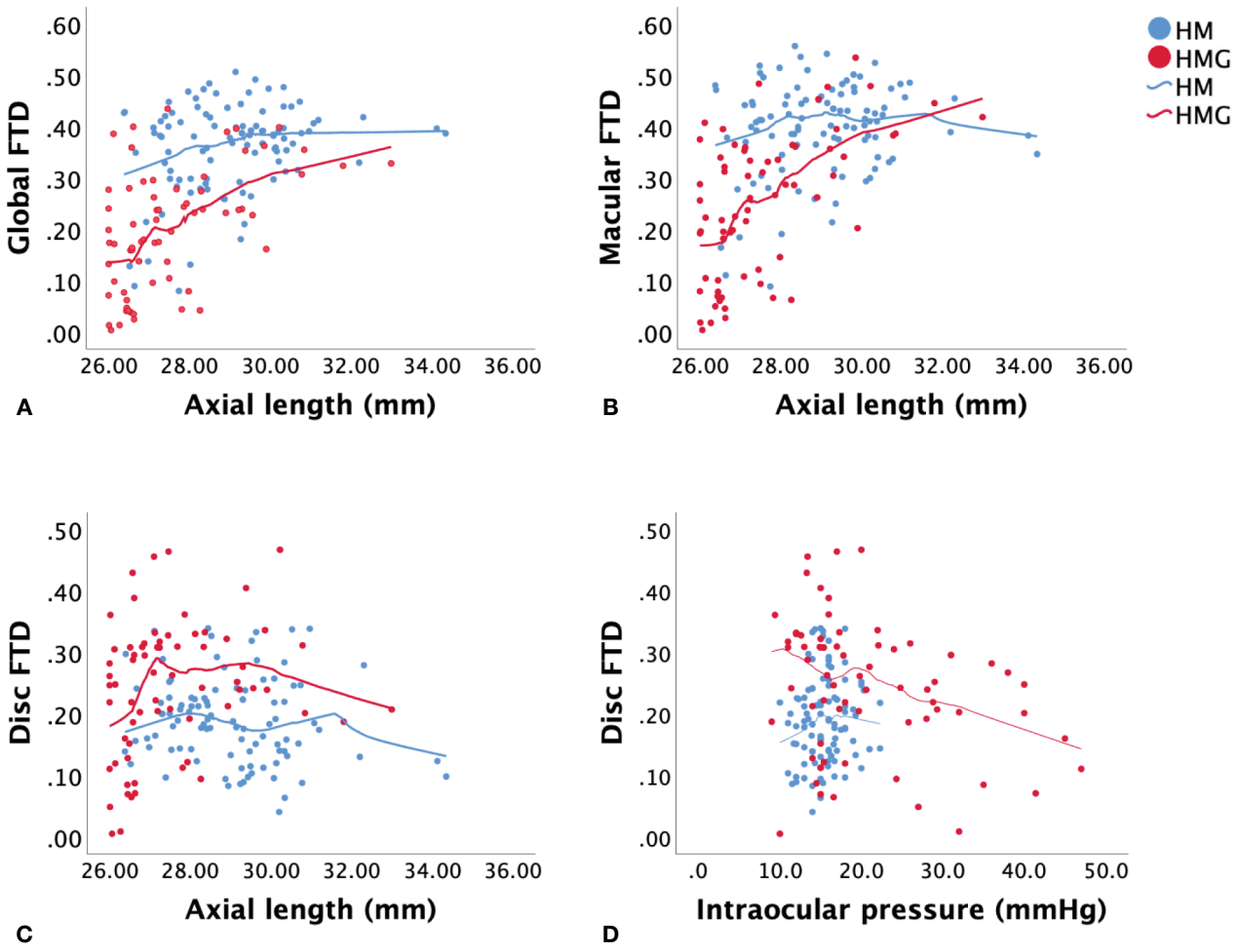

Figure 4. Scatter diagrams of FTD and associated factors in HM and HMG groups. The global FTD (**A**) macular FTD (**B**) and disc FTD (**C**) in association with axial length in both groups. The disc FTD (**D**) in association with IOP in both groups.

interesting phenomenon of marked but intermediate FT because of a sudden increase in IOP was observed by Yan et al.[12] during tightening of the encircling band. However, the pathophysiology could be different from that of an eye with a high IOP for a long time, as in the present study participants. There may be several explanations for the present results, as follows: first, the long-term stress of high IOP could induce retinal edema, thus reducing the visibility of FT; second, high IOP in the eye might result in the thinning or reduced intensity of large choroid vessels; and third, the location and size of posterior staphyloma may be different between the HM and HMG groups, resulting in different clinical manifestations of FT. In addition, no significant correlations of optic disc parameters, including VCDR and DOI, were found with most of the FTDs in either group, except the macular region in the HM group. These results were similar to those of a study in patients with primary OAG showing that the optic disc shape in the tessellated group was not different from that in the non-FT group.

According to these results, the PPA was larger in eyes with HM than in eyes with HMG. A positive VPDR–global FTD correlation was found in both groups, whereas positive HPDR–macular FTD and VPDR–macular FTD correlations were found in eyes with HM and HMG, respectively. The present results were consistent with those of previous studies showing a correlation between a larger PPA and a higher FT,[12] but the previous studies did not investigate the direction of PPA and its association with FT. Since the eye is vertically stretched with increasing AL, the correlation between VPDR and FTD seen in the present results is reasonable. The PPA region is characterized by large choroidal vessels and the sclera under ophthalmoscopy and is composed of Bruch's membrane, but not the retinal pigmented epithelium and choriocapillaris, based on optical coherence tomography and

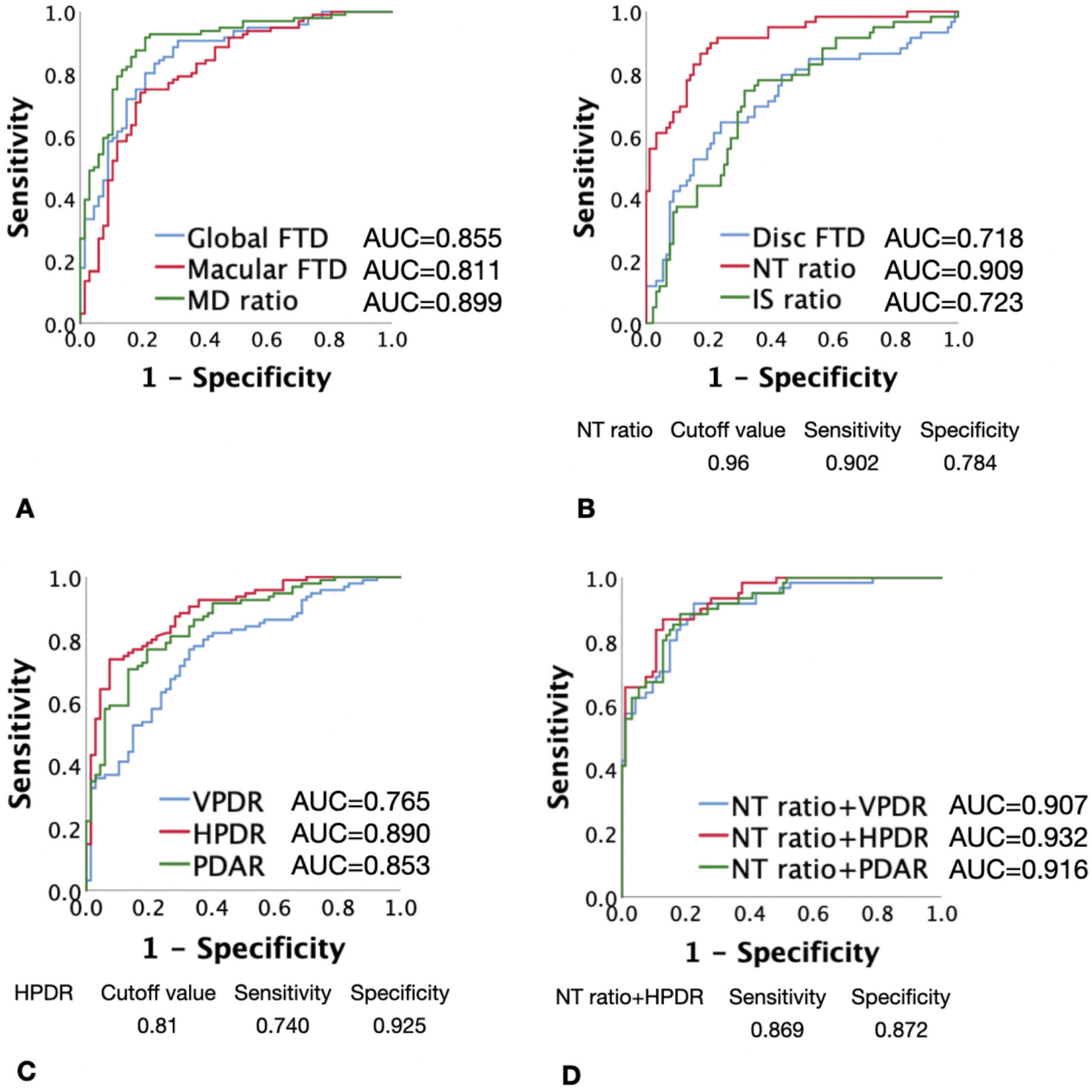

Figure 5. ROC curves used to evaluate FTD- and PPA-related parameters in the differential efficiencies of HM and HMG. (**A**) ROC curve and AUC for global FTD, macular FTD, and MD ratio. (**B**) ROC curve and AUC for disc FTD, NT ratio, and IS ratio. NT ratio had the highest AUC among FTD-related parameters. (**C**) ROC curve and AUC for VPDR, HPDR, and PDAR. HPDR had the highest AUC among PPA-related parameters. (**D**) ROC curve for NT ratio + VPDR, NT ratio+ HPDR, and NT ratio + PDAR. NT ratio + HPDR had the highest AUC among all the FTD- and PPA-related parameters. ROC, receiver operating curve; NT ratio, nasal FTD/temporal FTD ratio; IS ratio, inferior FTD/superior FTD ratio.

histological studies. Yan et al.[12] hypothesized that choroidal thinning, especially in the choriocapillaris, was the shared mechanism for the development of both PPA and FT. Therefore, based on our results and previous findings, we postulated that common choroidal thinning in the nasal region resulted in a larger HPDR in HM eyes, thus making HPDR the parameter with the highest differential efficacy between HM and HMG among other PPA-related parameters.

RVD was slightly but significantly higher in eyes with HMG than in eyes with HM and was negatively correlated with global and regional FTD in eyes with HM but not in eyes with HMG. Long-term stress of high IOP may have caused the insignificance of

RVD with FTD in the HMG group. These results also indicate the importance of retinal blood flow in maintaining fundus structure during myopic progression. Therefore, RVD may be a protective factor for myopic macular degeneration. This is consistent with a previous study on optical coherence tomography angiography showing significantly reduced vessel densities in the Category 2 fundi and suggests potential cell loss in the inner retinal layers.[36] Further, Huang et al.[17] found a positive correlation of greater FTD with vessel density inside the optic disc, but not between FTD and peripapillary retinal perfusion. These studies showed that blood flow varies in various locations; therefore, compensation during myopic maculopathy could be complex.

Our study had several strengths. First, we applied an objective and quantitative method to assess FTD based on artificial intelligence. The method was fully automated and was minimally influenced by the experience of ophthalmologists and different understandings of the FT among doctors. Second, all images were normalized and standardized during preprocessing to minimize the influence of image quality. Third, our results provide preliminary information on the intensity, distribution patterns, and parameters with differential efficiencies between the HM and HMG groups. Last, color fundus photography is advantageous for studying FTD compared with optical coherence tomography. However, this study had several limitations. First, the study was hospital-based and conducted at a single center, rather than being a population-based study. Moreover, owing to the retrospective nature of this study, we were unable to investigate our hypothesis on the speed of FTD development between the HM and HMG groups; thus, longitudinal studies are required. Third, use of IOP-lowering medications was not considered. Finally, our study results were limited to Category 1 and 2 fundi and are not suitable for including more advanced myopic degenerative fundus.

In conclusion, our study quantitatively assessed FTD in HM and HMG. Our results showed different FTD intensities, distribution patterns, and associated factors depending on the disease status, as well as the fundus regions analyzed, between eyes with HM and HMG. Since FTD and PPA are early signs of myopic shift, these results suggest different pathophysiology during disease progression between the two groups. Moreover, a higher macular NT ratio alone or in combination with a lower HPDR indicates a higher possibility of HMG than of HM. Our study proposed the potential value of FTD as a novel biomarker to diagnose glaucoma in high myopia. Future studies on the quantified FTD may predict the progression of the disease severity, and shed light on the possible mechanisms to the glaucomatous and non-glaucomatous visual field defect in HMG eyes.

Acknowledgments

The authors are thankful to the operators in the glaucoma examination room at Zhongshan Ophthalmic Center for their preparation of the fundus photographs.

Supported by the National Key R&D Project of China (2020YFA0112701); the National Natural Science Foundation of China (82171057); Science and Technology Program of Guangzhou, China (202206080005); Major Science and Technology Project of Zhongshan City (2022A1007).

Disclosure: **X. Chen,** None; **X. Chen,** None; **J. Chen,** None; **Z. Li,** None; **S. Huang,** None; **X. Shen,** None; **Y. Xiao,** None; **Z. Wu,** None; **Y. Zhu,** None; **L. Lu,** None; **Y. Zhuo,** None

* Xiaohong Chen, Xuhao Chen, and Jianqi Chen contributed equally as co-first authors.

References

1. Holden BA, Fricke TR, Wilson DA, et al. Global prevalence of myopia and high myopia and temporal trends from 2000 through 2050. *Ophthalmology*. 2016;123:1036–1042.
2. Wang YX, Yang H, Wei CC, et al. High myopia as risk factor for the 10-year incidence of open-angle glaucoma in the Beijing Eye Study. *Br J Ophthalmol*. 2023;107:935–940.
3. Modjtahedi BS, Abbott RL, Fong DS, et al. Reducing the global burden of myopia by delaying the onset of myopia and reducing myopic progression in children: the academy's task force on myopia. *Ophthalmology*. 2021;128:816–826.
4. Rezapour J, Bowd C, Dohleman J, et al. The influence of axial myopia on optic disc characteristics of glaucoma eyes. *Sci Rep*. 2021;11(1):8854.
5. Wang SK, Guo Y, Liao C, et al. Incidence of and factors associated with myopia and high myopia in chinese children, based on refraction without cycloplegia. *JAMA Ophthalmol*. 2018;136:1017–1024.
6. Hsu CH, Chen RI, Lin SC. Myopia and glaucoma: sorting out the difference. *Curr Opin Ophthalmol*. 2015;26:90–95.

7. Foo LL, Xu L, Sabanayagam C, et al. Predictors of myopic macular degeneration in a 12-year longitudinal study of Singapore adults with myopia. *Br J Ophthalmol*. 2023;107:1363–1368.
8. Fang Y, Yokoi T, Nagaoka N, et al. Progression of myopic maculopathy during 18-year follow-up. *Ophthalmology*. 2018;125:863–877.
9. Yan YN, Wang YX, Yang Y, et al. Ten-year progression of myopic maculopathy: the Beijing eye study 2001–2011. *Ophthalmology*. 2018;125:1253–1263.
10. Ohno-Matsui K, Kawasaki R, Jonas JB, et al. International photographic classification and grading system for myopic maculopathy. *Am J Ophthalmol.* 2015;159:877–883.
11. Spaeth GL. Development of glaucomatous changes of the optic nerve. In: Varma R, Spaeth GL, eds. *The Optic Nerve in Glaucoma*. Philadelphia: Lippincott; 1992:79.
12. Yan YN, Wang YX, Xu L, et al. Fundus tessellation: prevalence and associated factors: the Beijing Eye Study 2011. *Ophthalmology*. 2015;122:1873–1880.
13. Tan TE, Anees A, Chen C, et al. Retinal photograph-based deep learning algorithms for myopia and a blockchain platform to facilitate artificial intelligence medical research: a retrospective multicohort study. *Lancet Digit Health*. 2021;3(5):e317–e329.
14. Lu L, Ren P, Tang X, et al. AI-model for identifying pathologic myopia based on deep learning algorithms of myopic maculopathy classification and "plus" lesion detection in fundus images. *Front Cell Dev Biol*. 2021;9:719262.
15. Shao L, Zhang QL, Long TF, et al. Quantitative assessment of fundus tessellated density and associated factors in fundus images using artificial intelligence. *Transl Vis Sci Technol*. 2021;10(9):23.
16. Shao L, Zhang X, Hu T, et al. Prediction of the fundus tessellation severity with machine learning methods. *Front Med*. 2022;9:817114.
17. Huang D, Li R, Qian Y, et al. Fundus tessellated density assessed by deep learning in primary school children. *Transl Vis Sci Technol*. 2023;12(6):11.
18. Li R, Guo X, Zhang X, et al. Application of artificial intelligence to quantitative assessment of fundus tessellated density in young adults with different refractions. *Ophthalmic Res*. 2023;66:706–716.
19. Rezapour J, Proudfoot JA, Bowd C, et al. Bruch membrane opening detection accuracy in healthy eyes and eyes with glaucoma with and without axial high myopia in an American and Korean cohort. *Am J Ophthalmol*. 2022;237:221–234.
20. Lanca C, Sun CH, Chong R, et al. Visual field defects and myopic macular degeneration in Singapore adults with high myopia. *Br J Ophthalmol*. 2022;106:1423–1428.
21. Weinreb RN, Leung CKS, Crowston JG, et al. Primary open-angle glaucoma. *Nat Rev Dis Primers*. 2016;2:16067.
22. Zhang Y, Wen W, Sun X. Comparison of several parameters in two optical coherence tomography systems for detecting glaucomatous defects in high myopia. *Invest Ophthalmol Vis Sci*. 2016;57:4910–4915.
23. Brusini P, Johnson CA. Staging functional damage in glaucoma: review of different classification methods. *Surv Ophthalmol*. 2007;52:156–179.
24. Huang D, Qian Y, Yan Q, et al. Prevalence of fundus tessellation and its screening based on artificial intelligence in Chinese children: the Nanjing Eye Study. *Ophthalmol Ther*. 2023;12:2671–2685.
25. Wang M, Zhou X, Liu DN, Chen J, Zheng Z, Ling S. Development and validation of a predictive risk model based on retinal geometry for an early assessment of diabetic retinopathy. *Front Endocrinol (Lausanne)*. 2022;13:1033611.
26. Guo X, Li R, Lu X, et al. Quantization of optic disc characteristics in young adults based on artificial intelligence. *Curr Eye Res*. 2023;48:1068–1077.
27. Xu Y, Wang Y, Liu B, et al. The diagnostic accuracy of an intelligent and automated fundus disease image assessment system with lesion quantitative function (SmartEye) in diabetic patients. *BMC Ophthalmol*. 2019;19:184.
28. Chen H, Wen F, Li H, et al. The types and severity of high myopic maculopathy in Chinese patients. *Ophthalmic Physiol Opt.* 2012;32:60–67.
29. Koh VT, Nah GK, Chang L, et al. Pathologic changes in highly myopic eyes of young males in Singapore. *Ann Acad Med Singapore.* 2013;42:216–224.
30. Yoshihara N, Yamashita T, Ohno-Matsui K, Sakamoto T. Objective analyses of tessellated fundi and significant correlation between degree of tessellation and choroidal thickness in healthy eyes. *PLoS One.* 2014;9(7):e103586.
31. Warrow DJ, Hoang QV, Freund KB. Pachychoroid pigment epitheliopathy. *Retina.* 2013;33:1659–1672.
32. Switzer DW, Jr, Mendonça LS, Saito M, et al. Segregation of ophthalmoscopic characteristics according to choroidal thickness in patients with

early age-related macular degeneration. *Retina.* 2012;32:1265–1271.
33. Spaide RF. Age-related choroidal atrophy. *Am J Ophthalmol.* 2009;147:801–810.
34. Jonas JB, Gründler A. Optic disc morphology in "age-related atrophic glaucoma." *Graefes Arch Clin Exp Ophthalmol*. 1996;234:744–749.
35. Lin F, Qiu Z, Li F, et al. Macular and submacular choroidal microvasculature in patients with primary open-angle glaucoma and high myopia. *Br J Ophthalmol*. 2023;107:650–656.
36. Sun J, Wang J, Wang Y. Retinal Vasculature and microstructure in early dry-type myopic maculopathy. *J Ophthalmol*. 2019;2019:7540897.